Journal of Applied Polymer Science

Stepwise cure and properties of silicone resin for high-ultraviolet-transmission optical elements

Zhiyong Lv,[1] Chonggang Wu,[1] Jing Li,[2] Xiao Fang,[2] Dongdong Yu,[1] Huchuan Qin,[1] Peng Yu,[1,3] Xuhuang Chen[1,3,4]

[1]School of Materials Science and Engineering, Hubei University of Technology, Wuhan, Hubei 430068, People's Republic of China
[2]Huangpi Non-Commissioned Officer (NCO) School, Air Force Early Warning Academy, Wuhan, Hubei 430034, People's Republic of China
[3]Hubei Provincial Key Laboratory of Green Materials for Light Industry, Hubei University of Technology, Wuhan, Hubei 430068, People's Republic of China
[4]Collaborative Innovation Center for Green Light-Weight Materials and Their Processing, Hubei University of Technology, Wuhan, Hubei 430068, People's Republic of China
Correspondence to: X. Chen (E-mail: cxh213@126.com)

ABSTRACT: A new high-ultraviolet (UV)-transmission silicone-resin polymeric material was prepared via curing during hydrosilylation of tetramethyltetravinylcyclotetrasiloxane with tetramethylcyclotetrasiloxane by a liquid-surface supernatant method, using a stepwise heating program to avoid spontaneous combustion of the reaction mixture. The relationships were investigated in detail between reactive groups, cross-linking density, mechanical and UV-transmission properties. For this purpose, UV transmittance and dynamic mechanical properties, respectively, of the silicone resin were measured with UV–visible spectrophotometry and dynamic mechanical thermal analysis. In addition, surface roughness was evaluated with an atomic force microscope as well as an interferometer. The curing process was monitored by Fourier transform infrared spectroscopy and rotational rheometry. The cyclic silicone oils were compared with linear ones in structure and product properties. The results indicated that stepwise temperature control during curing process was particularly indispensible due to the presence of active Si—H bonds, and that the silicone resin of high modulus, high UV transmittance (92.7%) and low surface-roughness was largely homogeneous in cross-linking points distribution.
 J. Appl. Polym. Sci. **2016**, *133*, 43308.

KEYWORDS: crosslinking; optical properties; resins; structure–property relations; viscosity and viscoelasticity

Received 29 June 2015; accepted 3 December 2015
DOI: 10.1002/app.43308

INTRODUCTION

High-UV-transmission materials are essential to most analytical instruments and equipment such as UV optical components, delicate optoelectronic elements, UV-transparent sheets, etc.[1,2] Usually, they are mainly made of special inorganic glasses with high strength, small impurity content and low surface roughness. Silva *et al.*[3] studied the optical properties of a phosphate glass, P_2O_5–ZnO–Al_2O_3–BaO–PbO (PZABP), and found that the characteristic of this phosphate glass contributed to high transparency from 280 to 800 nm. However, the high-cost, process complication, and high energy-consumption have limited its wider applications; even reduction of the impurity content to lower light-scattering levels always is accompanied with stricter preparation conditions. Therefore, to research and develop polymer materials as its alternatives has become a challenging issue to be addressed. The research progresses of high-UV-transparency polymers have been reviewed by our group[4]: Yu *et al.*[5] prepared a polyimide/(silica–titania core–shell nanoparticle) hybrid thin film, whose transparency at 350 nm was found to be greater than 90%, and which could be used to prepare three-layer anti-reflective films on glass or PMMA-polymer substrates. Gu *et al.*[6] prepared thin films of metal–organic frameworks (MOFs) with and without ultrasonic bath, the results of which showed that the optical properties of the films had a close relationship with their surface characteristic, and that the light transmittances at visible region and 350 nm were almost 93% and 90%, respectively, upon the ultrasonic bath. Based on the considerations of cost, preparation technology and production cycle, silicone materials were selected as the new alternatives, which was primarily due to their reduced light absorption across UV region because of the lack of chromophores,[7,8] and to the fact that they can be easily prepared

through hydrosilylation reaction.[9] Transparent addition-type liquid silicone rubber (LSR), which was prepared by reaction of vinyl-terminated dimethyl silicone oil (≡Si—CH=CH_2) and hydrosilicone oil (≡Si—H) under catalysis of $H_2PtCl{\cdot}6H_2O$ in isopropyl alcohol, has become a popular material in the optoelectronic field over the past years due to its advantages of simple preparation, high manufacture efficiency, low cost, and energy saving.[10–12] For instance, solid–liquid coexistence gels or LSR with different strengths was obtained by controlling the contents of the reactive groups and thus the cross-linking density, which has widely been employed as cushioning or antiseismic materials in the fields of optoelectronic, electrical, and medical industries.[13,14] The aforementioned unreinforced addition-type LSR has usually adopted linear-structured silicone oils as the reactants, but generally turned out to be of poor mechanical properties. Vinyl MQ resin was considered to be the most effective modifier in terms of reinforcement of LSR,[15] but the UV transmittance at 350 nm of the reinforced product is modestly lower due to the occurrence of light scattering, which is caused by the addition of the third component, vinyl MQ resin, that has a mismatched shrinkage as well as a different refractive index (RI).

In this work, tetramethylcyclotetrasiloxane (D_4^H) and tetramethyltetravinylcyclotetrasiloxane (D_4^{Vi}) with cyclic structures have been chosen as the reactants to prepare high-UV-transmission materials. It is apparent that the D_4^{Vi} and the D_4^H can well be compatible because of their transparent appearances, identical backbone of Si—O—Si, and analogous structures. In addition, their comparable RIs (1.4342 vs. 1.4347 for D_4^{Vi} vs. D_4^H, respectively) give the product a uniform RI that can minimize light scattering effectively, and their nearly identical densities (0.986 vs. 0.987 g/cm^3 for D_4^{Vi} vs. D_4^H at 25°C, respectively) contribute to a complete mixing without the occurrence of stratification. Also, defoaming is unnecessary due to the low viscosities of the reactants, which can make bubbles disappear rapidly without adding an alkynol inhibitor to avoid introduction of impurities. This study focuses on a qualitative analysis of the D_4^{Vi}–D_4^H curing behavior via Fourier transform infrared spectroscopy (FTIR) combined with rotational rheometry. The dynamic mechanical properties, surface roughness, and UV-light transmittance, respectively, of the silicone resin obtain from D_4^{Vi}–D_4^H reaction are investigated by means of dynamic mechanical thermal analysis (DMTA), atomic force microscopy (AFM) and interferometry, and UV–visible (UV–Vis) spectrophotometry. A stepwise heating method, which conduces to controlling the reaction rate, as well as a liquid-surface supernatant method, which contributes to obtaining the product in any size or thickness, is employed for the preparation of the silicone resin.

EXPERIMENTAL

Materials

D_4^{Vi} (≥98%) and D_4^H (≥98%) were purchased from Shenzhen Osbang New Materials, China, the vinyl and hydrogen contents of which were 30.51 and 1.67 wt %, respectively. Pt catalyst used for the cure of D_4^{Vi}–D_4^H was obtained from Dongguan Honye Silicone, China, the concentration of which was 4000 ppm. Glycerin and toluene, both analytically pure, were obtained from Xilong Chemical, China and Shanghai Aladdin, China, respectively. Deionized water was prepared in our laboratory. Polytetrafluoroethylene (PTFE) mold as reaction vessel was customized from Shenzhen Yimei Hardware Plastic Products, China.

Stoichiometric Ratio

The cross-linking density and properties of the product are directly determined by the molar ratio of D_4^H to D_4^{Vi} during the reaction (i.e., the molar ratio of ≡Si—H to ≡Si—CH=CH_2 group), which was calculated according to the following equation:

$$\frac{M_{D_4^{Vi}} \times a\%}{27} \times A = \frac{M_{D_4^H} \times b\%}{1} \quad (1)$$

where $M_{D_4^{Vi}}$ and $M_{D_4^H}$ are the weights of D_4^{Vi} and D_4^H, respectively, a wt % and b wt % are the contents of vinyl group and hydrogen group, respectively, and A is the stoichiometric (molar) ratio of D_4^H to D_4^{Vi}. In consideration of the possible side reactions of Si—H groups,[16] all of the samples were prepared by using a 2:1 molar ratio of D_4^H/D_4^{Vi} to ensure that the vinyl groups be thoroughly consumed.

Preparation of the Silicone Resin

The standard formula (based on 100 parts by weight of D_4^H) for the preparation of the silicone resin was as follows: D_4^H, 100 p.h.r.; D_4^{Vi}, 74 p.h.r.; Pt catalyst, 0.5 p.h.r. Predetermined amounts of D_4^{Vi} and D_4^H according to this formula were mixed in a 200 mL stoppered round-bottomed flask under magnetic stirring at 20°C for 3 min, and the Pt catalyst was then added dropwise into the stirred mixture, followed by a stoppered mixing for another 5 min to isolate the system from air. Subsequently, the stepwise heating method was initiated as follows: (1) kept the reaction-mixture flask stand at 25.0 ± 0.1°C for 10 h, during which the viscosity of the mixture increased gradually while still maintained a viscous flow state; (2) the mixture was then poured into a PTFE-mold rectangular cavity of 50 mm in depth surface-covered in advance with a layer of glycerin of ca. 5 mm, and subsequently placed in a vacuum oven set at 40°C for 3 h, thus forming an LSR-like soft sheet, which was recovered and then surface-washed with deionized water to remove thoroughly the residual glycerin, and subsequently cut into different dimensions of specimens; (3) finally, the LSR specimens were further cured at 120°C for 1 h to form transparent, glass-like silicone-resin specimens for all of the measurements to be prescribed below.

Liquid-Surface Supernatant Method

The conventional method for preparing silicone materials is as follows: the rectangular mold-cavity is comprised of four slide glasses on a glass substrate, with the forming surfaces being four longer side-surfaces of the four slide glasses, respectively, and the surface of the glass substrate, and a polyimide film (of 0.13 mm thick) is placed between the glass substrate and the mold cavity to improve mold release. Leveling-off of the above mold cavity is effected by ensuring that the bubble is centered in the liquid of a spirit level, which, however, cannot be absolutely guaranteed due to the limits of the spirit-level precision and observation errors.

To overcome this, a home-made, innovative technique so-called "liquid-surface supernatant method" was developed in our laboratory for the preparation of leveled silicone sheets of uniform thicknesses. PTFE was used in place of glass to form the mold cavity, in that the excellent non-adhesion property and extremely low surface tension of PTFE[17] helped minimize the interfacial adhesion between the silicone sheet and the mold walls. Then, glycerin was selected as the bottom cladding of the PTFE mold due to its high boiling point, high density, colorless transparency and incompatibility with the reactive silicone mixture. Finally, the reactive mixture was poured slowly onto the glycerin surface upon standing at 25°C for 10 h, and any bubbles possibly generated during the process may be removed through the subsequence vacuuming at 40°C. By this procedure, the reaction mixture remained strictly self-leveled irrespective of the orientation of the PTFE mold due to the relatively low viscosity of glycerin under gravity. It was certain that any dimensions of silicone sheets could be prepared using this liquid-surface supernatant method, by adjustments of the amount of the poured reaction mixture and/or the shape and size of the PTFE mold-cavity.

Cure-Confirmation Tests

In the oscillatory shear mode, curves of complex-viscosity magnitude versus time at a strain amplitude of 0.5% and an angular frequency of 6 rad/s were measured on a rotational rheometer (TA Instruments, DHR-2) at 95, 100, and 105°C, respectively, for the uncured reaction-mixture sample of D_4^H, D_4^{Vi}, and the Pt catalyst. FTIR spectra were obtained from an FTIR spectrometer (Thermo Fisher Nicolet, iS50) for the uncured sample and the cured samples upon stepwise heating at 25°C for 10 h, at 40°C for 3 h, and at 120°C for 1 h, respectively. Both of the tests were to confirm the occurrence of the gradual curing behavior.

Cross-Linking Density Test

The cross-linking density of the completely cured sample upon the stepwise heating was measured by an equilibrium swelling method presented below: a certain amount of the sample was immersed into excess anhydrous toluene in a sealed vessel at 25.0 ± 0.1°C; upon swollen in the toluene for 6 days, the sample was taken out and weighed after blobed dry with tissue wipers. The weight of swollen sample (M_1) was taken as the median of five tested results to minimize statistical uncertainties.

The content of the cross-linking bonds as well as the structure of the cured system can be reflected by the cross-linking density measured.[18] According to the Flory-Rehner theory,[19] the cross-linking density (v_e) of the cured sample was estimated by the following equation:

$$v_e = \rho / M_c = -\left[\ln(1-\varphi) + \varphi + \chi\varphi^2\right] / \left(V_0 \varphi^{1/3}\right) \quad (2)$$

where ρ is the density of the (un-swollen) sample (1.115 g/cm^3), M_c (g/mol) the average molecular weight between cross-linking points, φ the volume fraction of silicone resin in the swollen sample, χ (here 0.465)[18] the Flory-Huggins interaction parameter between the solvent and the sample, and V_0 the molar volume of toluene (1.0654×10^{-1} L/mol). The φ in eq. (2) was calculated by:

$$\varphi = (M_0/\rho) / [M_0/\rho + (M_1 - M_0)\rho_s] \quad (3)$$

where M_0 and M_1 are the weights of the (un-swollen) sample (0.1364 g) and the swollen sample (0.1837 g), respectively, and ρ_s is the density of toluene (0.866 g/mL).

Hardness Test

Upon standing at 25.0 ± 0.1°C for 1 day, the stepwise cured sample (50 mm × 50 mm × 3.8 mm according to ASTM D 2240-2005 standard) was tested at six separated testing points using a Shore-D-type durometer (Qingdao Zongheng Instruments, China, Chuan Lu). The results had to be read in 1 s upon indentation of the sample points. The hardness value was average from the six results tested above.

Dynamic Mechanical Thermal Analysis (DMTA)

The DMTA of the (cured) silicone resin (59.74 mm × 13.22 mm × 3.54 mm) was conducted on a dynamic mechanical analyzer (TA Instruments, Q800). A temperature sweep test was run from 30 to 140°C with a heating rate of 3°C/min in the air atmosphere, in the oscillatory three-point bending mold at an amplitude of 15 μm and a frequency of 10 Hz according to ASTM D 5418-15. Storage modulus (G'), loss modulus (G''), and loss tangent (tan δ) were obtained as functions of temperature for analysis.

Surface Topography Tests

The surface roughness of the sample within an observation range of 10 μm × 10 μm was inspected by an atomic force microscope (Bruker, Dimension Icon) in the PeakForce QNM mode, which were also tested by a ZYGO interferometer (ZYGO, Mark III-GPI) in a 19 mm × 18 mm observation range and analyzed by the software of MetroPro 8.3.1.

UV Transmittance Test

The UV transmittance of a silicone-resin film (1 mm thick), prepared by the liquid-surface supernatant method, was detected by a UV–Vis spectrophotometer (Hitachi, U3900) in a wavelength range of 200–800 nm at a scan rate of 300 nm/min.

RESULTS AND DISCUSSION

Curing Behavior Analysis

The physical and mechanical properties of silicone materials were significantly influenced by their curing conditions.[20–22] In the process of curing, combustion and implosion was found to easily be triggered with violent exotherm, if the reaction mixture was cured directly at 120°C without using the stepwise heating method; the reaction mixture burst into ashes within seconds even in the absence of ignition. To accommodate the time–temperature superposition theory in terms of the curing effect, behaviors of complex-viscosity magnitude versus time were studied at 95, 100, and 105°C, respectively. As shown in Figure 1, the system viscosity remained almost unchanged (ca. 0.1 mPa s) in the early stage of 30–80 s, followed by a sharp increase which gradually slowed down until the end of the observation time, for each of the temperatures investigated. This suggests that the cross-linking may not have occurred during an induction period of 30–80 s, which is dependent upon the nature and the composition of the curing system[9,23] as well as the reaction conditions. After the induction, the viscosity

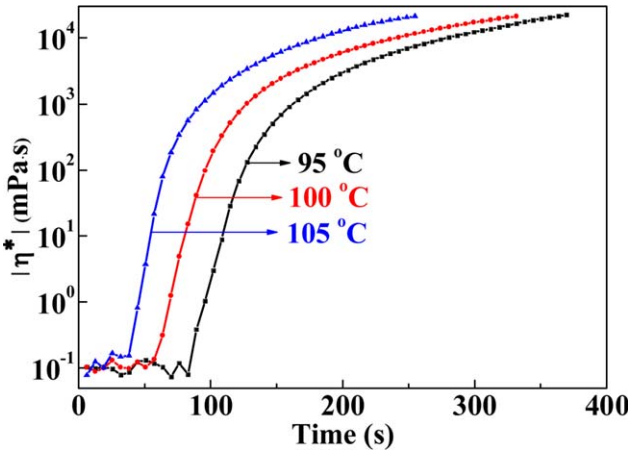

Figure 1. Rheological behaviors of complex-viscosity magnitude ($|\eta^*|$) vs. time at 95, 100, and 105°C for the reactive mixture of tetramethylcyclotetrasiloxane (D_4^H) and tetramethyltetravinylcyclotetrasiloxane (D_4^{Vi}). [Color figure can be viewed in the online issue, which is available at wileyonlinelibrary.com.]

increased considerably with time, indicating the significant occurrence of cure. During this process, the molecular thermodynamic movement and thus the molecular activity were enhanced upon the activation by the heat released from Si—H bonds oxidation, which resulted in vigorous growth in the viscosity and a sharp increase in the reaction rate. These rapidly cured products (within ca. 6 min) obtained from the isothermal treatments apparently were rough-surfaced, warped, corrugated, and bubbled, suggesting that the temperatures of 95–105°C were too high for the curing of the reaction mixture. However, it is obvious from Figure 1 that, as the curing temperature increased, the induction period decreased while the viscosity increased noticeably (at the same specified time), revealing that the cure rate was closely correlated with the temperature. Therefore, temperature control seemed to be the most effective way to prevent the reaction mixture from implosion.

Nevertheless, even though the curing temperature was decreased significantly to 35°C, the heat generated from the cross-linking and possible side reactions such as Si—H oxidation brought up some local temperatures to above the bubble point of the reaction mixture, giving rise to a great quantity of tiny bubbles existing in the cured product; this was undesirable for high-UV-transmission applications. Meanwhile, it was found that the flash point (T_f, the lowest temperature of flashover generated on the surface)[24] of organosilicon compounds can be evaluated by the following equation[25]:

$$T_f = -51.2385 + 0.4994T_b + 0.00047T_b^2 \quad (4)$$

where T_f and T_b are the flash point and the boiling point of organosilicon compounds, respectively. Through eq. (4), the T_f's of the D_4^H and the D_4^{Vi}, respectively, were estimated from their T_b's of 134 and 224°C to be 24.0 and 98.9°C, which was the reason why the curing temperature of 120°C, definitely higher than the T_f of the D_4^H–D_4^{Vi} reaction mixture, was sufficient to cause spontaneous combustion and even implosion. Further, according to the flash-point prediction models for flammable liquid mixtures,[26] the T_f of the mixture might have been lower than 35°C, which would potentially have made the reaction system take the hazards of quick polymerization accompanied by massive bubble formation at the curing temperature of 35°C. Generally, the flash point of compounds was determined by their volatility and boiling point. For those neither ionic nor nonpolar compounds, their molecules often contain permanent dipoles, which are determined by the electronegativities of the atoms in bonding: the larger the difference in electronegativity, the greater the dipolar moment.[27] A comparison of the molecular structures of D_4^H and D_4^{Vi} (Figure 2) reveals that the only difference was the reactive groups joined to Si atoms, i.e., H atoms for D_4^H vs. vinyls for D_4^{Vi}. The inconspicuous difference in Pauling value of electronegativity between Si and H atoms (1.89 for Si vs. 2.2 for H)[28] explains for the small dipolar-moment, low boiling point and low flash point of the D_4^H.

Therefore, an initial curing temperature as low as 25°C (i.e., room temperature) was applied for a prolonged time-period of 10 h that was apparently prior to the gelation of the system, follow by 40°C × 3 h and finally by 120°C × 1 h, which constituted a stepwise heating method to control the curing rate within a reasonable level that minimized bubbling, implosion, and spontaneous combustion. The corresponding FTIR spectra of the reactive mixture over four characteristic stages (Figure 3) show that: (1) across the entire process, the Si—O—Si absorption bands appeared in the range of 1300–950 cm^{-1};[29] (2) the two peaks at 2963 and 2906 cm^{-1}, respectively, corresponded to the asymmetric and symmetric C—H stretching vibrations from the —CH_3 groups; (3) the peak at 2167 cm^{-1} was the characteristic absorption band of the Si—H bonds; (4) the peaks at 1598 and 3056 cm^{-1} were attributed to the respective stretching vibrations of the C=C and C—H bonds from the vinyl groups. Compared with Spectrum *a* (unreacted low-viscosity state), a new peak in Spectrum *b* (reacted viscous-flow state) appeared at 1140 cm^{-1}, which was assigned to the C—C stretching vibration[30] resulting from the hydrosilylation of ≡Si—CH=CH_2 with ≡Si—H. The intensities of the peaks at 2167 and 1598 cm^{-1} both decreased monotonously in the order of Spectrum $a \rightarrow b \rightarrow c \rightarrow d$, confirming the progress of the curing reaction. Particularly at the end of cure (in Spectrum *d*), the absorption band at 1598 cm^{-1}, corresponding to the stretching of C=C

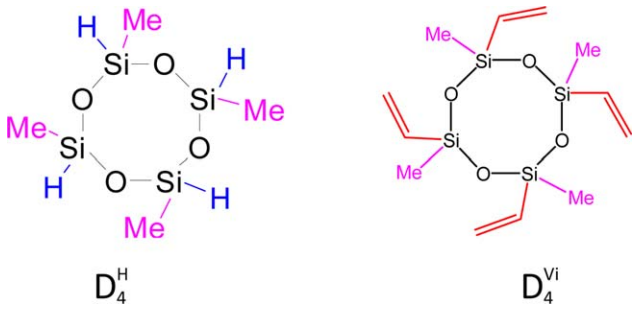

Figure 2. Molecular structures of tetramethylcyclotetrasiloxane (D_4^H) and tetramethyltetravinylcyclotetrasiloxane (D_4^{Vi}). [Color figure can be viewed in the online issue, which is available at wileyonlinelibrary.com.]

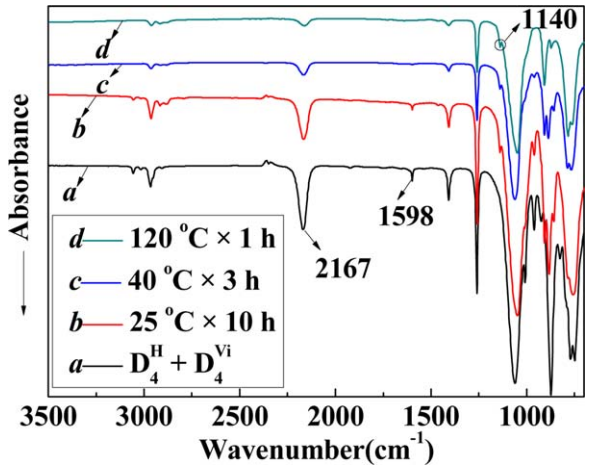

Figure 3. FTIR absorption spectra of the reactive mixtures of tetramethylcyclotetrasiloxane (D_4^H) and tetramethyltetravinylcyclotetrasiloxane (D_4^{Vi}) that are: (a) uncured; (b) cured at 25°C for 10 h; (c) cured at 25°C for 10 h followed by at 40°C for 3 h; (d) cured at 25°C for 10 h, followed by at 40°C for 3 h and finally at 120°C for 1 h. [Color figure can be viewed in the online issue, which is available at wileyonlinelibrary.com.]

bonds of the vinyl groups, was found to disappear, indicating that the curing reaction proceeded almost to completion.

Cross-Linking Density

In this work, the cross-linking density value (2.87×10^{-3} mol/cm^3) of the silicone resin (made from 30.51 wt % of vinyls contained in 74 p.h.r. of D_4^{Vi}), which was estimated during the equilibrium-swelling experiment by use of eqs. (3) and (4), is significantly (ca. one order of magnitude) higher than that of an LSR (2.65×10^{-4} mol/cm^3)[31] prepared by using a dosage of 0.30 wt % of vinyls contained in 46.0 p.h.r. of a linear vinyl silicone-oil (LVSO), and also considerably higher than that of an LSR modified by a branched vinyl silicone-oil (BVSO) (7.60×10^{-4} mol/cm^3) prepared in our previous work,[32] where the dosage was 2.25% of vinyls contained in 0.4 p.h.r. of a BVSO. This is primarily because the vinyl-group concentration applied in our reaction mixture obviously was much higher than those[31,32] mentioned above, the hydrosilylation of which under the catalysis of Pt catalyst accordingly led to an immensely higher cross-linking density. On the other hand, the molar ratio of 2:1 used for ≡Si–H/—CH=CH$_2$ was conducive to the complete consumption of the vinyl groups and thus the maximization of the highly cross-linked polysiloxane network.

Hardness Measurement

As shown in Table I, the shore-D hardness of the silicone resin (78.1) was compared with those of several thermoplastic resins,[33–36] which was found to be in close proximity to that of the un-plasticized PVC (80.3). This is mainly because the movement of the flexible silicone chains was "locked" gradually upon the progressive formation of cross-linking points: the more the cross-linking points formed, the stronger the chain intersegmental interactions, and thus the more rigid the cured-silicone chains. Moreover, unlike the flexible LVSO chains, the D_4^H and D_4^{Vi} silicone-oils was endowed by their cyclic structures with rigidity, as well as with thermostability in that cyclic-structure polysiloxanes are the end products of pyrolysis of their linear counterparts.[37] The structure of the silicone-resin product is represented in Figure 4, which apparently constituted a compact network.

Dynamic Mechanical Thermal Analysis (DMTA)

Figure 5 shows the dynamic mechanical properties (G', G'', and tan δ) of the silicone resin against temperature [G' and G'' vs. T are shown in Figure 5(a), and tan δ vs. T is shown in Figure 5(b)]. It is obvious that, in a specific temperature range of 30–140°C, G' of the silicone resin prepared from the cyclic-structured oils was so high as to be higher than that of the melt-blended material of 60 wt % of a silicone rubber (Dow Corning, Silastic NPC-40) and 40 wt % of a liquid-crystalline polymer, Vectra A 950 (with rigid rod-like molecular conformation and stiff backbone chains).[38] The mechanism for the high G' was similar to that for the high hardness. The glass transition temperature (T_g), taken as the temperature corresponding to the peak in a tan δ-vs.-temperature plot,[39] of the silicone resin (88.7°C) was higher than that (30°C) of liquid-crystalline reinforced LSR,[38] and much higher than those (−115 and −110°C, respectively) of an LSR and its composite reinforced by ethyoxyl-phenyl-POSS.[29] Nevertheless, its tan δ was of a lower value (0.067) than the LSR (0.138) and the composite (0.11); although the differences in topological structure between the silicone resin and the LSR and its composite might make their internal frictions (i.e., G''s) different as well, the higher tan δ of the former than the latter would essentially be dictated by its much too much higher G' since tan $\delta = G''/G'$. The high T_g of the silicone resin was primarily attributed to the rigidity of its chain segments comprising cyclic structural units. Unlike the LSR/vinyl-POSS composite with a T_g lower than room temperature, the chain movement of the silicone resin was restricted within a narrow space as a result of the extremely dense cross-links present; therefore, the silicone resin was in a "frozen" state at room temperature, that is, a higher temperature above its T_g was essential to make the molecular chains unfreeze to motion.

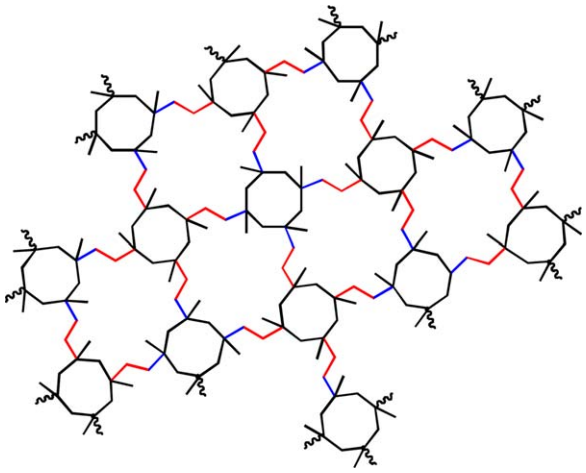

Figure 4. Schematic representation of the topological chain-structure of the 3D network for the silicone-resin product formed from the hydrosilylation of tetramethyltetravinylcyclotetrasiloxane (D_4^{Vi}) with tetramethylcyclotetrasiloxane (D_4^H). [Color figure can be viewed in the online issue, which is available at wileyonlinelibrary.com.]

Table I. Shore-D Hardness of the Silicone Resin (78.1) Compared with Those of Several Thermoplastic Resins

Hard materials	Silicone resin	PVC[33]	PLA[34]	POM[34]	PA6[35]	PC[36]	PC-A380-5[36,b]
Hardness (Shore D)	78.1[a]	80.3	81 ± 0.7	74 ± 0.5	72.0	56 ± 2.0	75 ± 2.0

[a] The STD value (0.09) of hardness was calculated from the six tested results.
[b] PC-A380-5 refers to the PC enhanced by 5% hydrophilic fumed silica with a surface area of 380 m2/g and average particle size of 7 nm.

Surface Topography Analysis

Figure 6 illustrates the 3D topography of silicone resin (i.e., an image of height vs. position coordinates) within a 10 μm × 10 μm observation range, from which the surface of the silicone resin was found to be molecularly smooth, showing the root mean square (RMS) and the average roughness (R_a) values of 1.74 and 1.39 nm, respectively. In addition, no local defect or uneven-shrinkage was visually present on the surface inspected. These probably were due to an appropriately mild control of the process conditions by the stepwise heating method to minimize internal stresses, which resulted in a uniform distribution of the cross-linking points as well as the formation of a homogeneous network structure. Figure 7 shows a section analysis across a 5 μm length in the observation range, from which we observed that the height fluctuations were only within ca. 8 nm, indicating further that the surface was really smooth enough both globally and locally. The low surface-roughness was further confirmed by ZYGO interferometry as shown in Figure 8; the peak-to-valley (PV) and RMS values were tested to be 1.108λ and 0.188λ (λ = 632.8 nm), respectively. The surface-roughness RMS value (1.74 nm) obtained from AFM of the silicone resin is even lower than that (6.91 nm) of the 1%-K–2%-Er codoped ZnO film,[40] which has widely been applied to UV-light emitters, transparent electronics, surface acoustic-wave devices, etc.[41] These results suggest that the internal stresses in the cured silicone resin, which were caused by nonuniform shrinkages and led to the variations in shape and size such as warpages, cracks, or corrugations, were nearly zero, upon the application of the stepwise heating method.

According to the "Curing behavior analysis" section, temperature control was crucial to the curing process. The stepwise heating method had to be applied to prevent sharp temperature changes and thus the occurrence of fast cure, as the curing behavior was completely temperature-sensitive. Across the whole stepwise curing from low-viscosity to viscous, to rubbery and to

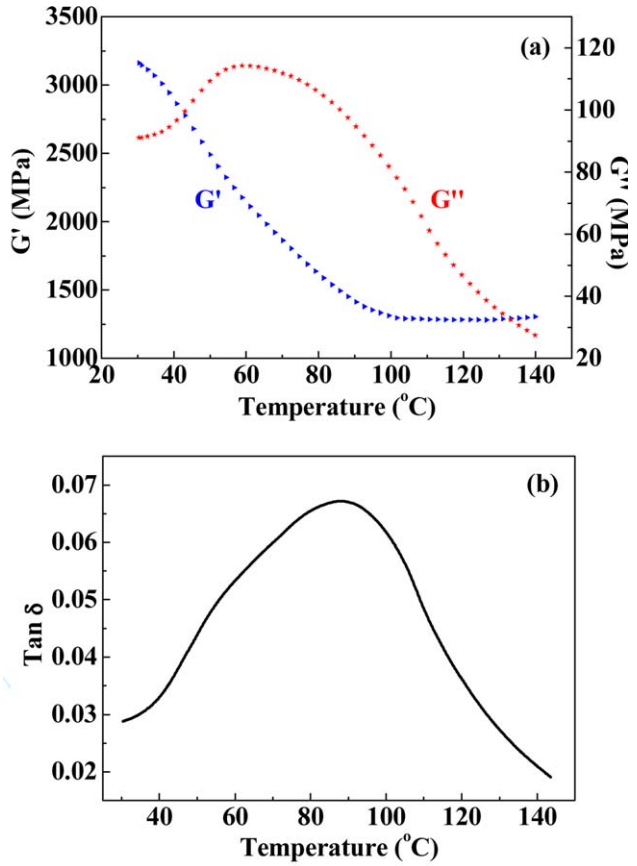

Figure 5. Dynamic mechanical properties (G', G'', and tan δ) of the cured silicone resin against temperature: (a) G' and G'' vs. T; (b) tan δ vs. T. [Color figure can be viewed in the online issue, which is available at wileyonlinelibrary.com.]

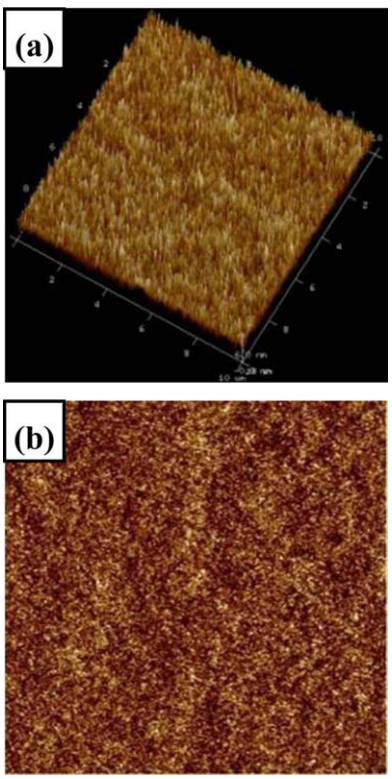

Figure 6. AFM surface topography of the cured silicone-resin sheet: (a) 3D image within a 10 μm × 10 μm observation range; (b) 2D top-view image. [Color figure can be viewed in the online issue, which is available at wileyonlinelibrary.com.]

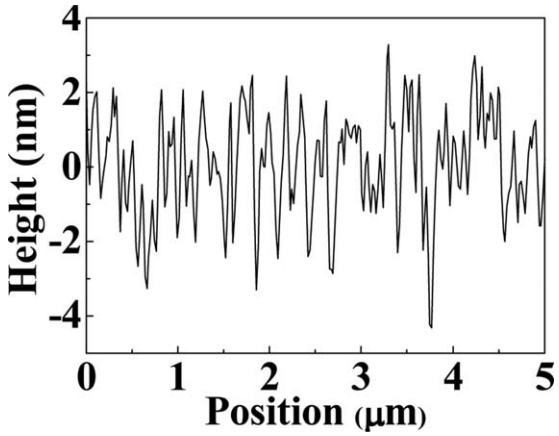

Figure 7. Section analysis from 3D image across a 5 μm length, i.e., a plot of height vs. position.

hardened state, the mild effects of temperature changes suppressed the emergence of surface defects resulting from nonuniform shrinkages.

UV Transmittance Measurement

The UV transmittances of the silicone-resin sheet in a wavelength range of 200–800 nm are shown in Figure 9, in which the transmittance at 350 nm was as high as 92.7%, which is higher than 85.3% at 350 nm for the silicone resin[42] synthesized through hydrolytic polycondensation of 1,3-dihydrotetramethyldisiloxane, methylvinyldimethoxysilane, dimethyldimethoxysilane, and phenyltrimethoxysilane and used for modification of epoxy resin in the field of optoelectronic packaging, especially for encapsulating light-emitting diodes (LEDs). Why did the silicone resin in our work accomplish such a high UV-transmission? Firstly, unsaturated chromophoric groups readily absorb the UV light to induce electron transition, which is the dominating factor that decreases the UV transmission[43]; however, as corroborated by the FTIR absorption spectroscopy, there were very little vinyl groups present in the cured end-product, which was realized by application of the stoichiometric ratio of 2:1 for ≡Si—H/—CH=CH_2 (i.e., an excess of ≡Si—H groups). Second, the number of components and the compatibility between components bring about light scattering; in this system, this issue was little involved, since D_4^H was reacted at a molecular level with D_4^{Vi} to form a homogeneously cured network. Thirdly, a rough surface would result in diffuse reflections of UV light in different directions; nevertheless, AFM and interferometry analyses revealed that the surface of the cured product was smooth enough (i.e., surface-roughness RMS values of 1.74 and 118.9 nm, respectively). Fourthly, nonuniform thicknesses could change the directions of light propagation, whereas the thickness uniformity of the silicone-resin sheet in this work was ensured by the liquid-surface supernatant method applied. These have made the D_4^H and D_4^{Vi} become the preferred starting materials to prepare high-UV-transmission optical elements, only upon simultaneous applications of the stepwise heating method for the cure and the liquid-surface supernatant method for the forming.

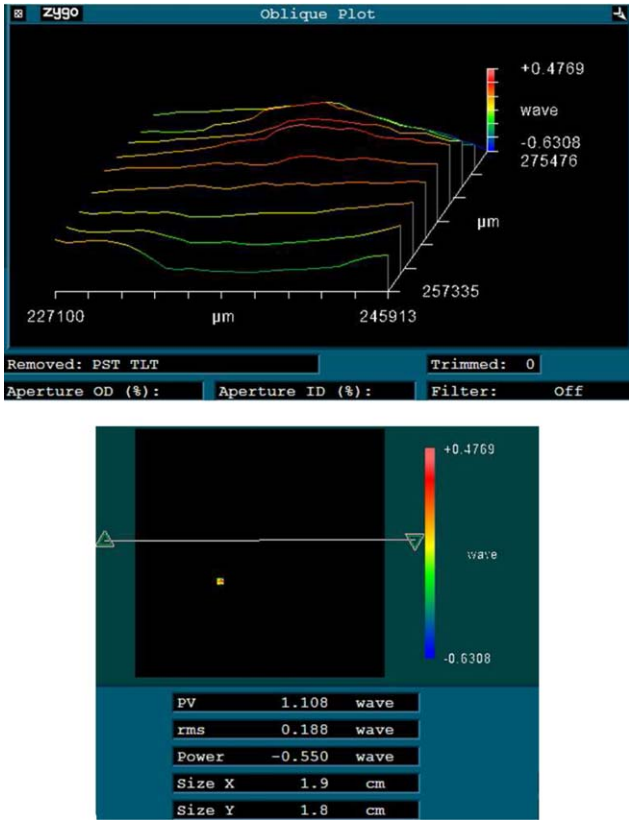

Figure 8. Peak-to-valley (PV) and root mean square (RMS) values of 1.108λ and 0.188λ ($\lambda = 632.8$ nm), respectively, for the surface-roughness evaluation of the cured silicone-resin sheet, obtained from ZYGO interferometry. [Color figure can be viewed in the online issue, which is available at wileyonlinelibrary.com.]

On the other hand, the UV loss at 350 nm of 7.3% for the sheet may be attributed to two factors. Firstly, the absorption band can easily be generated from the light-energy absorption of Pt

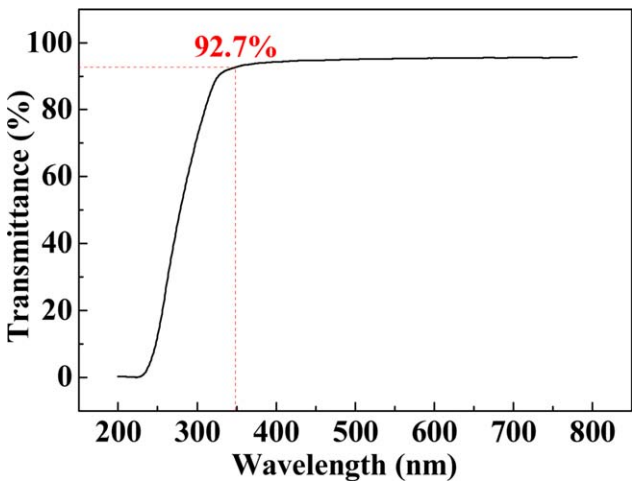

Figure 9. UV transmittances of the cured silicone-resin sheet in a wavelength range of 200 − 800 nm, showing a transmittance of 92.7% at a wavelength of 350 nm. [Color figure can be viewed in the online issue, which is available at wileyonlinelibrary.com.]

catalyst in UV region.[17,44] Second, even the mirror reflection from the sheet surface plays a role in decreasing UV transmittance.

CONCLUSIONS

In this work, tetramethylcyclotetrasiloxane (D_4^H) has been reacted with tetramethyltetravinylcyclotetrasiloxane (D_4^{Vi}) at a stoichiometric ratio of 2: 1 to produce a cured silicone-resin sheet of little residual vinyl groups, dense and uniform cross-links, high modulus and hardness, uniform thicknesses, smooth surface, and thus of high UV-transmission, using an innovative stepwise heating method for control of cure as well as a homemade liquid-surface supernatant method for control of forming. An excess of ≡Si—H groups is applied to ensure near exhaustive consumption of vinyl groups, which is evidenced by FTIR absorption spectroscopy. The stepwise heating method, i.e., 25°C for 10 h, follow by 40°C for 3 h and finally by 120°C for 1 h, realizes a homogeneous cure accompanied by little residual internal-stresses, and therefore smooth-enough surfaces of the cured sheet, as corroborated by AFM and interferometry. The liquid-surface supernatant method, i.e., superimposition of the D_4^H–D_4^{Vi} reactive mixture upon mobile, self-leveled glycerin, effects an absolute leveling-off state for either surface of the mixture, and thus uniform thicknesses of the cured sheet. These three process-conditions jointly contribute to the accomplishment of a high UV transmission at 350 nm of up to 92.7%, with the absence of unsaturated chromophoric groups such as vinyls the most contributive. As a material of high UV-transmission, the silicone-resin sheet thus formed finds applications in optical elements such as transparent films in optoelectronic devices. Promisingly, the UV loss by mirror reflection would be minimized by application of a silica anti-reflection coating onto the sheet surfaces in our future studies.

REFERENCES

1. Yang, B.; Wang, Q.; Zhang, W. H.; Ouyang, S. Y.; Zhang, Y. P. *J. Lumin.* **2015**, *158*, 390.
2. Huang, T.; Hu, Z. G.; Xu, G. S.; Zhang, X. L.; Zhang, J. Z.; Chu, J. H. *Appl. Phys. Lett.* **2014**, *104*, 111908.
3. Silva, G. H.; Anjos, V.; Carmo, A. P.; Pinheiro, A. S.; Dantas, N. O. *J. Lumin.* **2014**, *154*, 294.
4. Chen, X. H.; Chen, X. T.; Lu, J.; Xing, W. G. *Mater. Sci. Eng.* **2014**, *30*, 182.
5. Yu, Y. Y.; Chien, W. C.; Tsai, T. W.; Yu, H. H. *Mater. Chem. Phys.* **2011**, *126*, 962.
6. Gu, Z. G.; Pfriem, A.; Hamsch, S.; Breitwieser, H.; Wohlgemuth, J.; Heinke, L.; Gliemann, H.; Woll, C. *Micropor. Mesopor. Mater.* **2015**, *211*, 82.
7. Shit, S. C.; Shah, P. *Natl. Acad. Sci. Lett.* **2013**, *36*, 355.
8. Ojima, I. In *The Chemistry of Organic Silicon Compounds*; Patai, S.; Rappaport, Z., Eds.; Wiley: New York, **1989**; Vol. *2*, Chapter 25, p 1479.
9. Marciniec, B.; Gulinski, J.; Urbaniak, W.; Kornetka, Z. W. Comprehensive Handbook on Hydrosilylation; Marciniec, B., Ed.; Pergamon: Oxford: **1992**; p 116.
10. Cai, D.; Neyer, A. *J. Microelectromech. Syst.* **2010**, *19*, 1362.
11. Lucile, L.; Vincent, G.; Guillaume, B. *Opt. Mater.* **2014**, *37*, 352.
12. Gu, Q. G.; Zhou, Q. L. *Eur. Polym. J.* **1998**, *34*, 1727.
13. Qin, Y. X.; Fu, J.; Yu, L.; Yang, Z. R.; Guo, W. Y. *Adv. Mater. Res.* **2013**, *641*, 333.
14. Bae, J. Y.; Kim, Y. H.; Kim, H. Y.; Kim, Y. B.; Jin, J. H.; Bae, B. S. *ACS Appl. Mater. Interfaces* **2015**, *7*, 1035.
15. Chen, D. Z.; Chen, F. X.; Hu, X. J.; Zhang, H. W.; Yin, X. Z.; Zhou, Y. S. *Compos. Sci. Technol.* **2015**, *117*, 307.
16. Voronkov, M. G.; Pukhnarevich, V. B. *Russ. Chem. Bull.* **1982**, *31*, 939.
17. Park, B. H.; Lee, M.; Kim, S. B. *Appl. Surf. Sci.* **2011**, *25*, 3709.
18. Vieyres, A.; Albouy, P. A.; Sanseau, O. *Macromolecules* **2013**, *46*, 889.
19. Flory, P. J.; Rehner, J. *J. Chem. Phys.* **1943**, *11*, 512.
20. Hong, I.; Lee, S. *J. Ind. Eng. Chem.* **2013**, *19*, 42.
21. Li, B.; Zhang, Z. D.; Ma, D. P.; Zhai, Q. Q.; Feng, S. Y.; Zhang, J. *J. Appl. Polym. Sci.* **2015**, *132*, DOI: 10.1002/app.42656.
22. Hernández-Ortiz, J. P.; Osswald, T. A. *J. Appl. Polym. Sci.* **2011**, *119*, 1864.
23. Stein, J.; Lewis, L. N.; Gao, Y.; Scott, R. A. *J. Am. Chem. Soc.* **1999**, *121*, 3693.
24. Hshieh, F. *Fire Mater.* **1997**, *21*, 277.
25. Wang, G. B.; Chen, C. C.; Liaw, H. *J. Ind. Eng. Chem. Res.* **2011**, *50*, 12790.
26. Phoon, L. Y.; Mustaffa, A. A.; Hashim, H.; Mat, R. *Ind. Eng. Chem. Res.* **2014**, *53*, 12553.
27. Nagle, J. K. *J. Am. Chem. Soc.* **1990**, *112*, 4741.
28. Suresh, C. H.; Koga, N. *J. Am. Chem. Soc.* **2002**, *124*, 1790.
29. Shi, Y. H.; Huang, G. S.; Liu, Y. P.; Qu, Y. B.; Zhang, D.; Dang, Y. *J. Polym. Res.* **2013**, *20*, 1.
30. Fang, W. Z.; Zeng, X. R.; Lai, X. J.; Li, H. Q.; Chen, W. J.; Zhang, Y. *J. Thermochim. Acta* **2015**, *605*, 28.
31. Xu, Q.; Pang, M. L.; Zhu, L. X. *Mater. Des.* **2010**, *31*, 4083.
32. Yin, Y. L.; Chen, X. T.; Lu, J.; Chen, X. H. *J. Rubber Res.* **2014**, *17*, 161.
33. Unar, I. N.; Soomro, S. A.; Aziz, S.; Pak, J. *Anal. Environ. Chem.* **2011**, *11*, 44.
34. Clarizio, S. C.; Tatara, R. A. *J. Polym. Environ.* **2012**, *20*, 638.
35. Baena, L.; Jaramillo, F.; Calderon, J. A. *Fuel* **2012**, *95*, 312.
36. Luyt, A. S.; Messori, M.; Fabbri, P.; Mokofeng, J. P.; Taurino, R.; Zanasi, T.; Pilati, F. *Polym. Bull.* **2011**, *66*, 991.
37. Michalczyk, M. J.; Farneth, W. E.; Vega, A. *J. Chem. Mater.* **1993**, *5*, 1687.
38. Shivakumar, E.; Das, C. K.; Pandey, K. N. *Macromol. Res.* **2005**, *13*, 81.
39. Scott, C.; Ishida, H. *J. Mater. Sci.* **1991**, *26*, 5078.

40. Vettumperumal, R.; Kalyanaraman, S.; Thangavel, R. *Superlattices Microstruct.* **2015**, *83*, 237.

41. Norton, D. P.; Heo, Y. W.; Lvill, M. P.; Pearton, S. J.; Chisholm, M. F.; Steiner, T. *Mater. Today* **2004**, *7*, 34.

42. Zhang, Y.; Yang, X.; Zhao, X. J.; Huang, W. *J. Appl. Polym. Sci.* **2012**, *61*, 294.

43. Pavlikov, A. V.; Gayduchenko, I. A.; Timoshenko, V. Y. *Microelectromech. Eng.* **2012**, *90*, 96.

44. Sircoglou, M.; Bontemps, S.; Bouhadir, G.; Saffon, N.; Miqueu, K.; Gu, W. X.; Mercy, M.; Chen, C. H.; Foxman, B. M.; Maron, L.; Ozerov, O. V.; Bourissou, D. *J. Am. Chem. Soc.* **2008**, *130*, 16729.